



Contents lists available at ScienceDirect

## Journal of Manufacturing Processes

journal homepage: [www.elsevier.com/locate/manpro](http://www.elsevier.com/locate/manpro)

Technical Paper

## Effect of mold compliance on dimensional variations of precision molded components in multi-cavity injection molding

Rasoul Mahshid<sup>a,\*</sup>, Yang Zhang<sup>b</sup>, Hans Nørgaard Hansen<sup>b</sup>, Alexander Henry Slocum<sup>c</sup><sup>a</sup> Department of Mechanical Engineering, Faculty of Engineering, University of Isfahan, Isfahan 81746-73441, Iran<sup>b</sup> Department of Mechanical Engineering, Technical University of Denmark, Lyngby, Denmark<sup>c</sup> Department of Mechanical Engineering, Massachusetts Institute of Technology, Cambridge, MA, United States

## ARTICLE INFO

## Keywords:

Error source  
 Displacement sensor  
 Precision injection molding  
 Thermal error  
 Warpage  
 Mold misalignment

## ABSTRACT

Precision injection molding of high performance components requires primary error sources affected the molded component to be identified and isolated such that these errors can be reduced if needed. To systematically isolate and quantify the contribution of misalignment, thermal variation and component warpage to the accumulated error observed on the component, a methodology is presented and tested around an existing mold which produced parts with high dimensional variability. The mold featured two concentric guide pillars on opposite sides of the parting plane and rectangular centering block elements at three locations. Mold displacements at the parting plane were measured through the incorporation of three eddy-current linear displacement sensors. Thermal error sensitivity was investigated using FEM simulations such that the induced variability from thermal expansion and filling phase was identified and quantified. Finally, molded component warpage was isolated and quantified, again by the means of FEM simulation. The results were confirmed by using the mold on two injection molding machines to produce an array of parts whose key dimensions were measured.

## 1. Introduction

Beginning in the late 1990s, researchers began investigating how various parameters affect the feasibility of producing a product with the desired manufacturing quality and intricacy. Manufacturing quality is basically conformance to specifications to produce quality products. As research progressed, it has been found that dominant parameters can be categorized into three levels: machine variables (such as temperature, pressure and motion), process variables (such as melt temperature, melt pressure, rate of heat dissipation and cooling) and quality definitions (or final response, such as shrinkage, warpage, part weight and part thickness) [1]. Many efforts have been made using sensors for mold temperature [2–4], cavity pressure [4,5], holding pressure [6,7] and clamping force (relevant energy consumption) [8] by which quality of molded parts were assessed. Monitoring the momentary separation of mold core and cavity plates has been found to have significant effect on variation of part weight in an online monitoring system for injection-molding process to achieve consistent part quality [9,10]. In 2003, Min discovered that indirect control variables such as part weight and nozzle/cavity pressure can be used as decision-parameters for monitoring the quality of molded parts in process [11]. Chen et al.

developed a capacitive transducer for continuous and real-time monitoring of in-mold flow front position and velocity while correlating over-packing and molded part weight with sensor outputs [12]. Moreover, Dubai et al. worked out a predictive controller for accurate monitoring and tracking screw position and velocity on an injection molding machine using linear potentiometer transducer to improve the product quality, reduce the number of rejects and increase the productivity (shorter injection time) in precision molding [13]. Lu and Gao reported on the effectiveness and feasibility of a stage-based quality control scheme where part weight and length control were selected as an online quality assurance when manipulating nozzle pressure, barrel temperature, and mold temperature [14]. Gordon et al. indicated that the most important process data is obtained from in-mold sensors, where the collected information is the nearest to the state of the polymer forming the final product [15]. For this study, melt temperature and pressure were used to obtain melt velocity and viscosity when taking into account finished part thickness, width, length, weight, and tensile strength as quality metrics. While the study by Kuek verified the utility of cavity pressure as a process indicator with a significant effect on the part quality [5], the study by Tsai and Lan found that a pressure sensor installed inside the cavity can make the molded part defective and

\* Corresponding author.

E-mail address: [r.mahshid@eng.ui.ac.ir](mailto:r.mahshid@eng.ui.ac.ir) (R. Mahshid).<https://doi.org/10.1016/j.jmapro.2021.04.048>

Received 12 September 2020; Received in revised form 4 January 2021; Accepted 20 April 2021

Available online 28 April 2021

1526-6125/© 2021 The Society of Manufacturing Engineers. Published by Elsevier Ltd. All rights reserved.

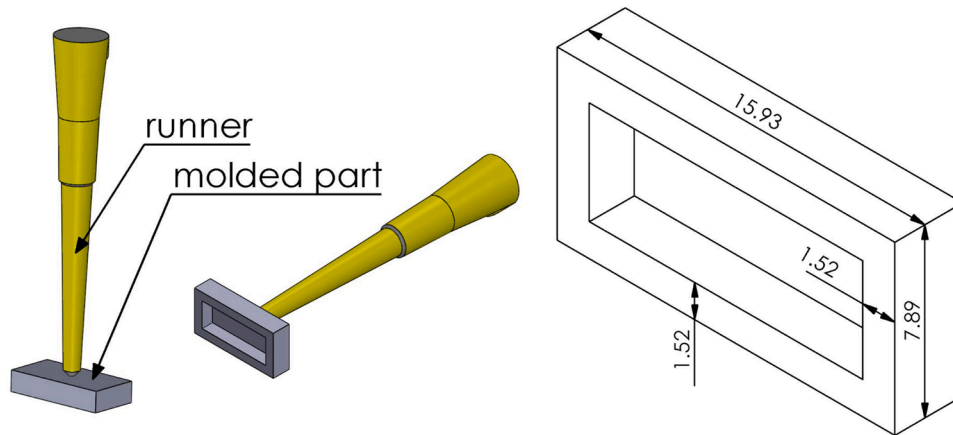


Fig. 1. Geometry and dimensions (in mm) of molded part.

investigated the correlation between melt pressure in different runner positions and cavity pressure where the runner pressure can represent the cavity pressure [16]. Since the use of extra sensors within the mold is costly to the manufacturer and increases efforts for mold making, Zhang et al. proposed a statistical quality monitoring method using only hydraulic pressure and screw position data obtained from built-in machine sensors [17]. Recently, Kitayama et al. replaced conventionally constant packing pressure with a packing pressure varying in the packing phase when minimizing warpage and cycle time as product quality variables (final response) and productivity respectively [18]. Additionally, Masato et al. demonstrated that melt temperature and packing pressure can alter dimensional variations between the part and the final part to a great extent [19].

In this manuscript, “displacement” is defined by the relative position of two molding plates in one direction ( $x$  or  $y$ ), caused by the motion of one plate or both plates; whereas “misalignment” is defined by the total relative displacement caused by movement of mold plates in  $x$  and  $y$  directions. Among parameters which affect dimensional precision of molded parts, displacement of the mold plates and misalignment between mold plates will lead to inaccurate replication or even failure. In fact, variations of few micro meters in molded parts may be enough to scrap it.

Clamping and cavity pressure during filling and packing stages, temperature gradient at the end of cooling and mold alignment feature kinematics are primary sources to deflect the mold from its intended configuration. When the mold is not compliant or exactly constrained, deflections and misalignment of platens may cause high levels of stress, leading to increased wear over the life of mold. In 2006, Carpenter et al. quantified both mold deflection during an injection molding cycle and the effect of machine compliance on mold behavior [20]. Niewels et al. disclosed a method and apparatus to counter mold deflection and misalignment using active material elements in an injection mold [21]. Huang et al. presented a method to measure real-time mold deflection during injection molding using inductive displacement sensors [22]. In 2014, Huszar et al. indicated the existence of core misalignment and noticeable core shifting and deflection by wall thickness measurements taken on the cross-sectioned molded parts [23]. While not fully convincing, evidence to control core shifting by altering the hydraulic pressure, proved to be efficient to reduce the thickness discrepancies arising from core deflection. Recently, in 2018 Jung and Lee developed and applied a numerical model to a center-gated disc model while investigating both melt flow behavior and effect of thermal expansion when revealing the dominant influence of thermal expansion in accurate prediction of mold deformation [24].

These previous studies indicate that in-process mold deformation due to machine compliance, packing pressure and thermal expansion can alter dimensional precision among molded parts, in some cases resulting in parts that do not meet the tight tolerance requirements common in complex applications. Furthermore, the effect of mold deflection on the molded parts needs to be quantified while differentiating the causes of dimensional variations. Therefore, if an in-process measurement to both molded parts and injection molds can be developed, there is the potential to significantly improve process efficiency by predicting in-process mold deflection and decreasing maintenance time.

The aim of this study is thus to obtain an insight into the effect of mold compliance on the precision of molded parts. This research quantifies the mold misalignment through incorporation of displacement sensors and examines if dimensions of molded parts are altered by the mold displacement or deformation. Previous studies have indicated the usage of different varieties of displacement sensors in online quality control for injection molding by monitoring mold separation and screw position (linear variable differential transformer sensors) [10,25,26], core-back distance and rate (laser displacement sensors) [27]. In particular, the causes of dimensional variations are addressed. To examine this possibility, in-process measurements are performed on mold platens using eddy-current sensors as an online monitoring technique while tracking changes of part dimensions for a number of cycles. The distance (displacement) between probes installed on stationary mold plate and target (movable mold plate) is thus detected accurately by measuring the AC resistance of the excitation coil which depends on the magnitude of the opposing field and eddy current [28,22]. The errors related to mold misalignment, thermal expansion and residual stress build-up in the molded parts are thus isolated and quantified. In addition, the warpage is one of the severe defects found in injection molding affecting dimensional variations of molded parts [29–32]. To address this undesired effect, there have been various research efforts aimed at optimizing parameters (process and machine variables) to minimize or even eliminate distortion and warpage for improving dimensional variations in mass production [33–36].

Numerical modeling is used to analyze the deformation of mold plates and warpage of the injection molded parts, which are believed to be the major reasons for dimensional deviation (from nominal value). For the mold testing, two injection mold machines were used to assess possible machine effects on molded parts. By following this approach and by understanding the magnitude of the variability induced by each error component, mold performance can be greatly improved at the design stage or by alterations to the existing mold and molding parameters.

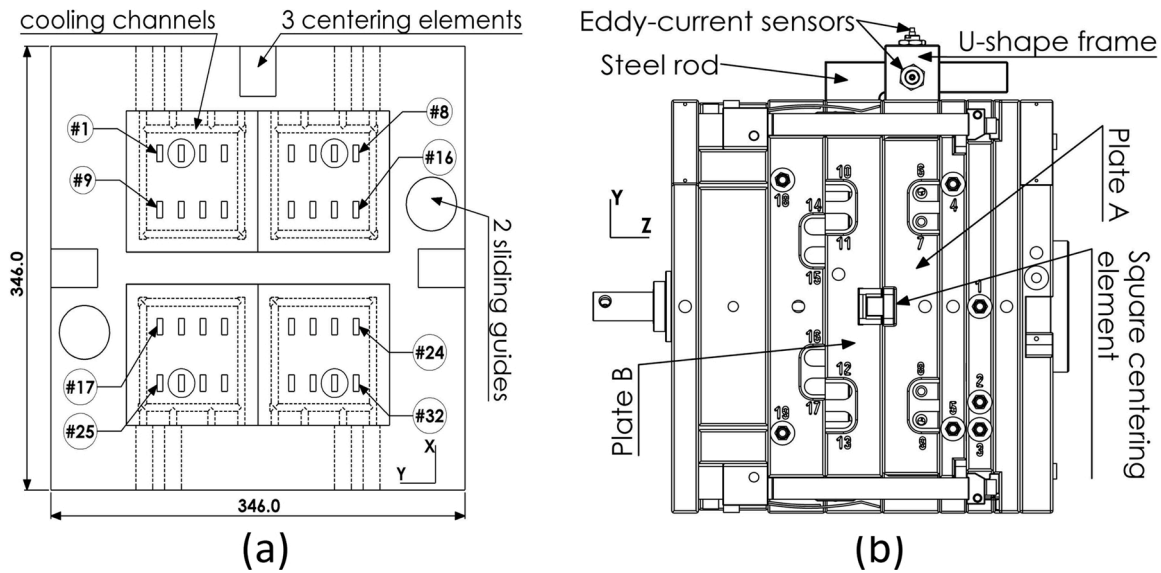


Fig. 2. Schematic of the testing mold (a) front view; (b) side view (dimensions in mm).

Table 1  
Process parameter settings on the molding machines.

Parameter	Values
Melt temperature	238 °C
Mold temperature	30 °C
Clamping force	280 kN
Packing pressure	100 bar
Injection velocity	75 mm/s
Cycle time	16 s
Cooling time	8 s
Filling time	1 s

## 2. Experimental setup and methodology

### 2.1. Injection mold and molded part

The geometry of the mold’s cavity and core in a production grade injection mold is illustrated in Fig. 1 with dimensions by the molded part, which is a thin walled box. A three-plate mold was used to perform the experiments. The mold cavity retainer plate includes four inserts where each has eight cavities. In total 32 plastic elements were produced at each cycle. The mold’s dimensions are 346 (mm) × 346 (mm) × 313 (mm) and it has 230 kg weight. In addition, the centering system in the mold is provided by standard guide elements which are used widely in punching and plastics industry by toolmakers. These includes two round sliding guides (centering pillar and bush) and three rectangular centering elements to ensure alignment of the mold halves. While the former has a total clearance of 9–25 μm, the latter allows precise alignment with a total clearance of 7–12 μm. These tolerances come from manufacturer’s specifications [37,38]. The details and schematic of the testing mold are illustrated in Fig. 2. For tracing the molded parts in different cycles, cavities have unique numbers. The material used in the injection molding machine and simulations is ABS (Terluran GP-35).

### 2.2. Molding procedure

The mold was installed on two injection molding machines: a Ferromatik Milacron K60 (in the following abbreviated IMM1) and an Arburg Edrive 470 (in the following abbreviated IMM2). The former is a hydraulic 600 kN machine while the latter is a fully electric 1000 kN machine. The process parameters applied on the injection molding machines are listed in Table 1. The testing includes running the mold on

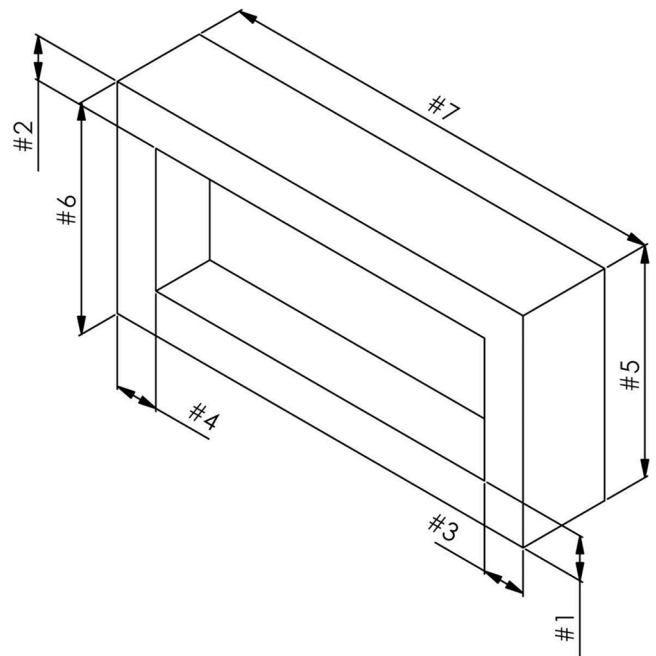


Fig. 3. Measuring points on the molded parts.

the machines in two conditions: with plastic injection and without plastic injection. At both conditions, displacement measurements for detection misalignment were performed on the front cavity (Plate A) and rear cavity (Plate B) plates as shown in Fig. 2.

### 2.3. Measurements

To observe possible misalignment effects, dimensions of the molded parts and mold plates displacement were measured. This could enable tracing back the parts’ dimensional errors to the mold’s displacement.

#### 2.3.1. Molded parts

A ZEISS PRISMO (single probing) of ZEISS coordinate measuring machines (CMM) was used in combination with ZEISS CALYPSO to ensure reliable measurements of parts’ dimensions. There are 4 wall



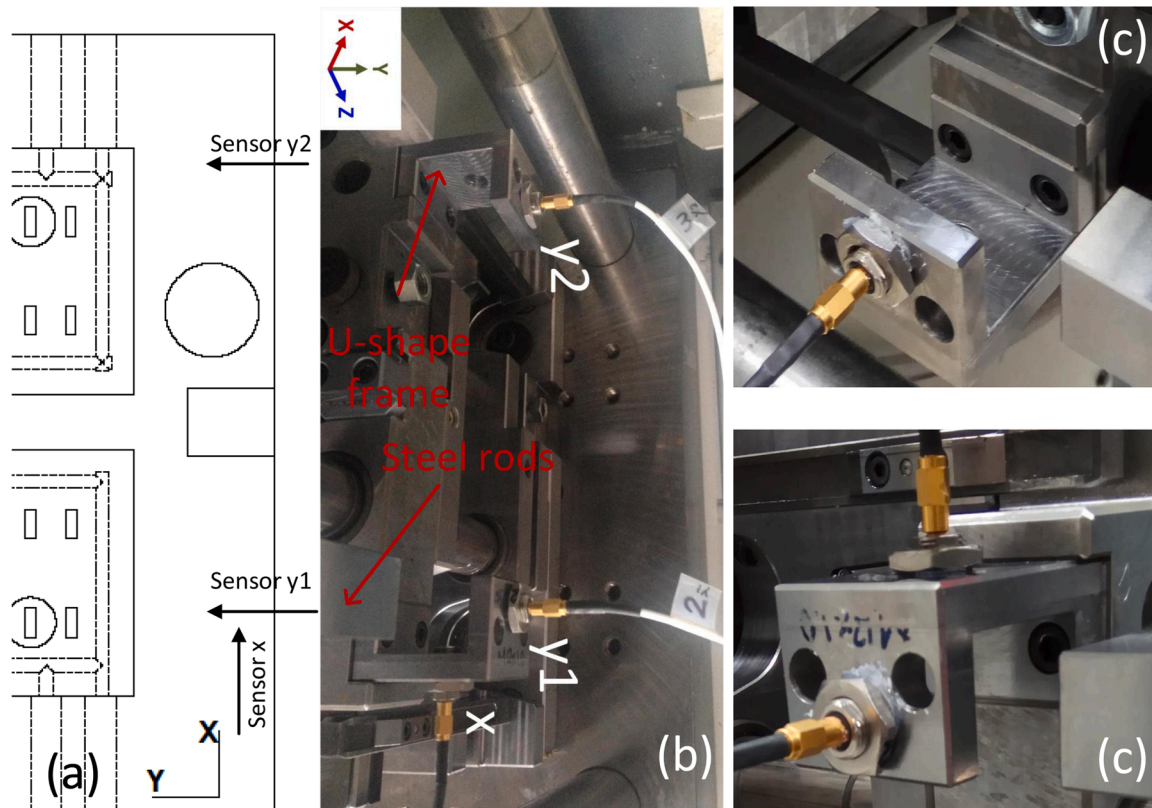


Fig. 4. Mounting sensors with threaded bodies and locking nuts: (a) Schematic view; (b) experimental setup; (c) sensor mounts with hot glue to lock mounting threads.

thicknesses, the outer length and width of the molded parts at two positions for measurements as illustrated in Fig. 3. The parts were collected at different cycle numbers. But they are from cavity numbers, 2, 7, 26 and 31 according to the layout shown in Fig. 2. In the figure, small circles highlights the cavities for part collection. The possible displacements for the mold's cavities in the parting plane are in x and y directions plus rotational motion around z axis. When occurring displacements for the mold's plates, they are the same for all cavities due to translational motion. However, when changing the orientation of plates, the molded parts in cavities at the farthest end of the plates indicate higher errors on their dimensions. In addition, the centering system (two round sliding guides and three rectangular centering elements) constrain the displacement and deformation of the mold's plates and cavity inserts. Therefore, a cavity from all four inserts was selected to get information on possible dimensional changes all around. Furthermore, while not

shown, the same experiments were conducted for cavity numbers 5, 8, 13, 16 and 17, 20, 25, 28 that belong to the inserts in upper right and lower right of the mold's plate respectively as shown in Fig. 2. However, when compared the dimensional variations on molded parts associated with these cavities to those selected in this research, the same or less dimensional variations were observed.

### 2.3.2. Mold

For displacement measurements on the mold, three non-contact eddy current probes were used. The system consists of three sensors, two U-shape frames and two steel rods. The sensors are from Micro-Epsilon (DT3010-S2-M-C3) with static resolution of 0.1 μm and measuring range of 2 mm. U-shape frames and sensors are installed on Plate A (stationary plate) while the steel rods are on Plate B (movable plate). When the rods move in front of the sensors, while closing and opening

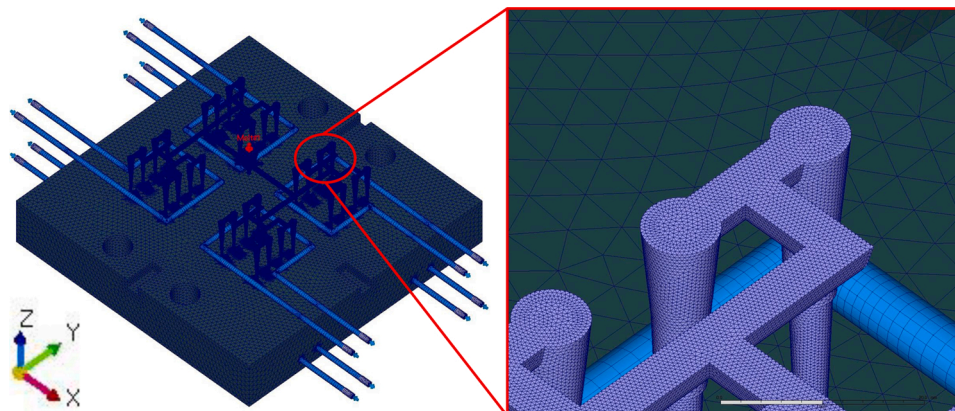


Fig. 5. 3D model and mesh for the whole mold; Left: entire model; Right: mesh for runner, cooling channel and mold insert.

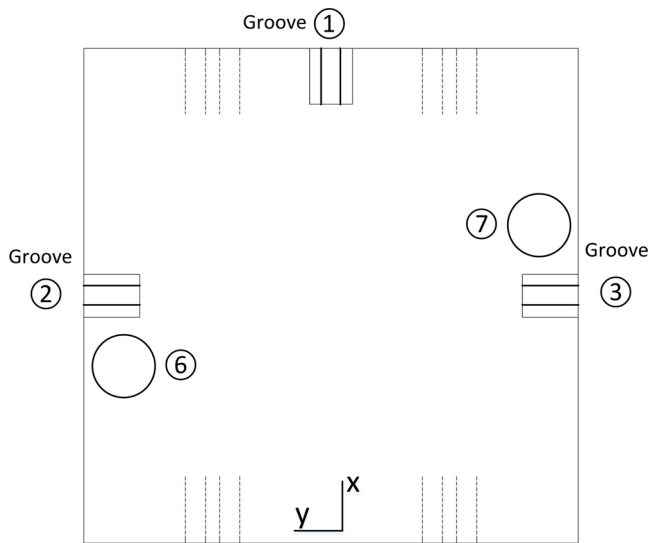


Fig. 6. Numbering of centering elements.

Table 2  
Boundary conditions applied to the nodes.

Nodes	Fixed (0 mm) at
6, 7	x, y
1	y
2, 3	x
Back of plates	z

the mold, they monitor the real-time displacement between the plates. The entire setup schematic can be observed in Fig. 2. When detecting x displacement at one end of plate, two sensors (y1 and y2) measure y variations at the both ends of plate. Therefore, the movements of plates with respect to each other were determined for displacements x, y and rotation around z axis. The entire arrangement of sensors and the mold can be viewed in Fig. 4.

2.4. Finite element modeling

For testing possible effects of mold thermal expansion on the misalignment of corresponding cores and cavities, the educational version of Moldex3D software with the implementation of the mold deformation was used to simulate the injection molding process and predict mold displacement errors. Mesh matching technique and equal mesh were employed on all contact surfaces in order to allow for mold deformation analysis. Due to the non-symmetrical geometry and boundary conditions (centering elements), a full 3D simulation of the mold was performed including runner, molded parts, cooling channels and the two mold plates. To obtain good resolution of the results, mesh type 5 Layers BLM with boundary layer offset ration 2 on the parts, mesh type 5 Layers BLM with boundary layer offset ration 1 on the runner, mesh type 3 Layers BLM with boundary layer offset ration 0,4 on the cooling channels and pure tetrahedral elements on the mold inserts were applied. The entire model and mesh for the runner, cooling channel and mold insert are illustrated in Fig. 5 (Plate A and cavity retainers are turn off to make the parts and runner visible). As previously mentioned, the material used in the molding machines and simulations was ABS.

The process parameter settings in all simulations were the same as those applied on the injection molding machines as listed in Table 1. Analyze sequence settings were assigned according to Transient Cooling, Filling, Packing, Transient Cooling, Warpage and Mold Deformation in all simulations. Mold displacement has two common error sources in injection molding. During the filling and packing phases, the high

Table 3  
Summary of testing conditions.

Name	Injection molding machine	Injection
T0	IMM1	No plastic
T1	IMM1	Plastic
T2	IMM2	Plastic

injection pressure from mechanical machines induces mold deformation. In addition, temperature gradients in the mold inserts result in thermal expansion causing dimensional variations of the final parts. Moldex3D is capable of modeling mold deformation to some extent. The module includes the effect of cavity pressure during the filling stage and mold temperature distribution at the end of cooling. It becomes apparent that Moldex3D does not consider cavity pressure caused by the packing phase. From FE simulations, it is shown that the packing phase created lower cavity pressure for this research due to the special design of the melt entrance. To obtain an accurate analysis of mold deformation, appropriate setting of the boundary conditions was needed to be employed for each cavity and core plates. With respect to centering element numbering shown in Fig. 6, displacements were fixed (0 mm displacement) on the appropriate nodes in x, y, z directions as listed in Table 2.

2.5. Methodology

The testing procedure consisted of running the mold at different experimental conditions with respect to the molding machines and injection molding cycles while displacement sensors were present in all tests. For each testing condition, molded parts were collected at cycles mostly with the same sampling interval. To verify repeatability of the results, the measuring procedure was replicated 5 times for each sample and the average values were used in graphs. Since the mold used was an actual production mold loaned for this research, technical drawings and tolerances were not available (proprietary). The nominal values which were calculated through Boolean operations as shown in Fig. 1 were considered as a reference for the parts measurements. Dimensional deviations are presented in the results to indicate how much and in which direction displacement errors occurred during the test. The most significant point to be made from dimensional variations is that it is possible to trace the dimension of the molded parts back to machine elements such as mold thermal expansion or misalignment of cavity and core plates.

In order to more exactly determine thermal effects on displacement of the mold plates, baseline tests were run while injecting no plastic into the mold when reading data by the displacement sensors. The rest of testing included running the mold with plastic injection while applying other testing conditions.

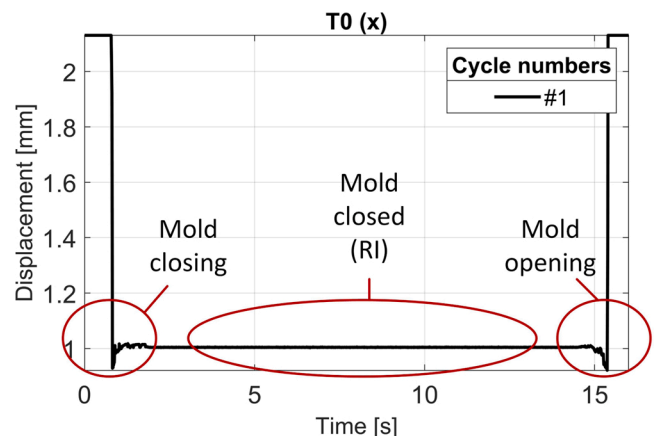


Fig. 7. The entire measurements obtained from sensors during one cycle (T0).

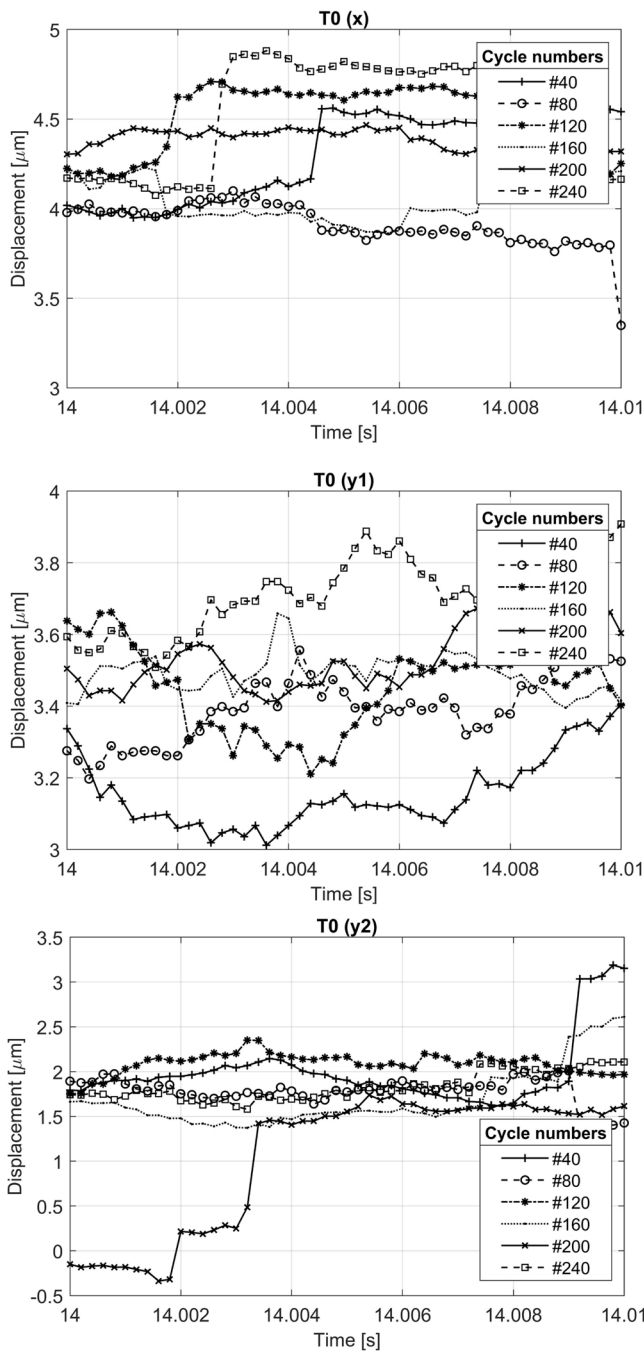


Fig. 8. Mold's plates displacement – T0.

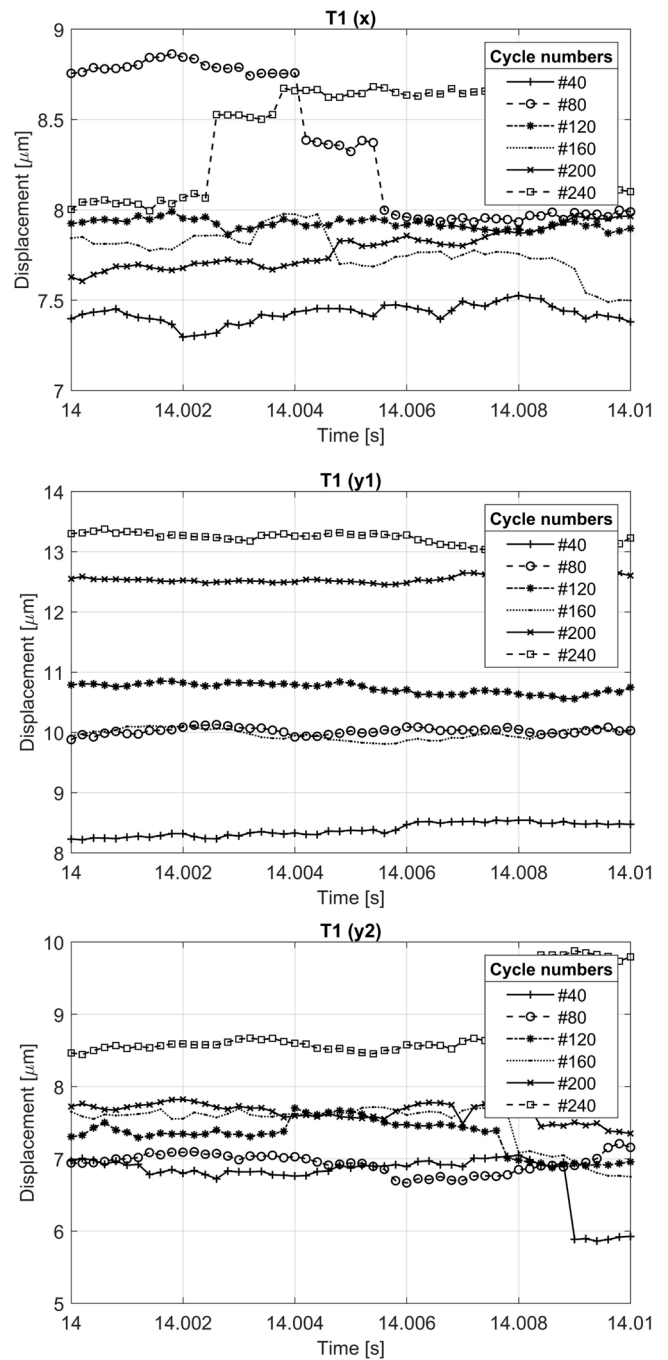


Fig. 9. Mold's plates displacement – T1.

To examine possibility of any complex mold deformation which could not be detected by displacement sensors, FE analysis was used with the same process parameters setting applied to injection molding machines. From the analysis, the effect of warpage on part dimension was explored if similarities can be found. Table 3 summarizes all the testing conditions and gives specific name to each to be referred more convenient in the following sections.

### 3. Results and discussion

Herein, the effects of different testing conditions (Table 3) on mold plates and dimensional variation of molded parts are compared to each other.

#### 3.1. Testing with no plastic injection (T0)

The first test was to run the mold for 260 cycles with no plastic injection. In this test, the actual temperature of the mold is constantly 30 °C. The three sensors measured mold displacement every tenth cycle. As previously mentioned, the purpose of this test was to ensure that the mold centering elements work appropriately and there are no large gaps or wear. The representative graph of the entire mold displacement recorded by the sensors within a mold cycle is shown in Fig. 7 and it is the same for x, y1 and y2 directions.

In the graphs, the horizontal axis shows the time where the sensors record the positions. In this case, with 5k samples/s, there is 80,000 samples in a cycle which is equivalent to 16 s. In addition, the front face



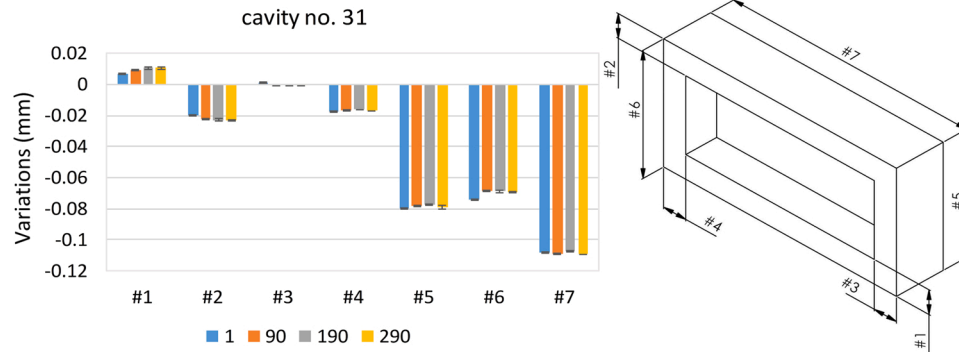


Fig. 10. Dimensional variations in cavity no. 31 – T1, error bars =  $\pm 1$  standard deviation, Max. standard deviation =  $1.2 \mu\text{m}$ .

of sensors on Plate A are placed in 1 mm distance to the rods on Plate B (Fig. 2) where the best precision is expected from the sensors according to the manufacturer's recommendation when the total measuring range is 2 mm. However, this is not practical when locking the sensors on the mold using hot glue, mounting threads and a nut as shown in Fig. 4. The sensor is fixed with a slight deviation from 1.0000 mm and the measured values by the sensors has the format 1.xxxx. When viewing the displacement graphs in this section, this 1 mm is subtracted from the measured values which are shown in  $\mu\text{m}$  on the vertical axis. While variability was found to exist on the dimensions of molded parts between a number of cycles, the variability of the mold displacement were deemed to be important for the purpose of this research. Therefore, when interpreting these images, the maximum deviation between the curves shown in a graph is considered as the real mold displacement which could affect the dimensional changes on the molded part.

It is also important to note that, although the figure shows the entirety of measurements of the mold's surfaces, the region of mold closed is the only region of interest (RI). Therefore, while not shown the whole RI, a portion of this region just before mold opening at cooling stage is shown for three sensors. When applying testing conditions T0, the displacement curves for representative cycles are shown in Fig. 8. When viewing the displacement profiles in Fig. 8, the centering elements of the mold held a maximum misalignment of 1, 2 and 4  $\mu\text{m}$  along x, y1 and y2 respectively.

### 3.2. Testing with plastic injection (T1)

The next series of tests were run with plastic injection for 290 cycles. The sensors recorded the displacement for each direction in every 10 cycles. The representative curves of the mold's plates displacement behavior are shown in Fig. 9. In examining the graphs, it is apparent that the plastic injection led to more misalignment as the displacement between the two mold's plates increased to 2, 6 and 6  $\mu\text{m}$  along x, y1 and y2 respectively.

In order to observe dimensional variations of this test, plastic parts were collected for cavity numbers 2, 7, 26, 31 at cycle numbers 1, 90, 190 and 290. While slight variability was found to exist between dimensional errors in all cavities, the representative graph of cavity 31 is shown in Fig. 10. When comparing the average errors from only one measuring point to each other, the same amount of variation over time was observed. Therefore, increasing the number of cycles had no effect on dimensional errors in this test. Likewise, when considering the changes in all measuring points, it is apparent that the error for wall thickness was less than 20  $\mu\text{m}$ , while this was around a maximum of 100  $\mu\text{m}$  for outer dimensions of the workpiece.

### 3.3. Testing with plastic injection (T2)

In total, 720 shots were performed for this test and plastic elements were collected every 30 cycles. As was done previously for T1 testing, the first measurements examined correspond to the displacement of the mold's plates. The representative plots can be seen in Fig. 11. As can be seen, the application of the new injection molding machine increased the misalignment between the plates with overall displacement of 7, 10 and 9  $\mu\text{m}$  along x, y1 and y2 respectively. This displacement causes more deviation in dimensions of plastic parts.

The dimensional variation analysis for this test was also conducted in the same manner as the T1 tests. The plastic elements were selected from cycle numbers 5, 120, 270, 390 and 570 when parts from cavity 2, 7, 26 and 31 were measured for each cycle. Once again, due to the similarity of results at all cavities, the representative graph is shown for cavity 31 in Fig. 12. The average length error was determined to be a maximum of 120  $\mu\text{m}$  at measuring point 7. As can be seen, the use of IMM2 slightly increased the error of part's dimensions for measuring points 5, 6. A maximum variation of 20  $\mu\text{m}$  was also observed in wall thicknesses from the graph. Therefore, IMM2 did not improve the part's error and it had slight negative effect on the dimensions of molded elements. In addition, while the error in wall thicknesses were found to be the same for both tests T1 and T2, the displacement sensors on the mold's plates in T2 proved to measure more effectively that the misalignment occurred during the injection molding process. Since the walls are formed between core and cavity sides of injection mold, the dimensional variations of wall thickness play an important role to indicate the misalignment of mold's plates. Furthermore, a tolerance of 10–15  $\mu\text{m}$  on mold inserts (cavities) is expected during machining process. This was reported by the mold maker and confirmed by the manufacturer of five-axis machine that was used to machine the mold components [39]. This leads to the conclusion that the misalignment in the mold is of the order of 10  $\mu\text{m}$ , while the milling and finishing processes in manufacturing procedure of mold insert are responsible for the rest.

### 3.4. FE analysis

As was shown in previous sections, two groups of dimensional errors in the molded parts were evaluated: wall thickness and outer dimensions. While the error was often below 20  $\mu\text{m}$  in the former, for the latter it varied from 60 to 120  $\mu\text{m}$ . This is a notable amount which cannot be neglected for the purpose of quality products of the molded parts.

To provide more detailed analysis of the process effect on mold's misalignment, a complete plastic injection molding simulation was conducted using Moldex3d when the mold base and mold inserts were present in the analysis. The analysis included filling, cooling (average), packing, cooling, mold deformation and warpage.

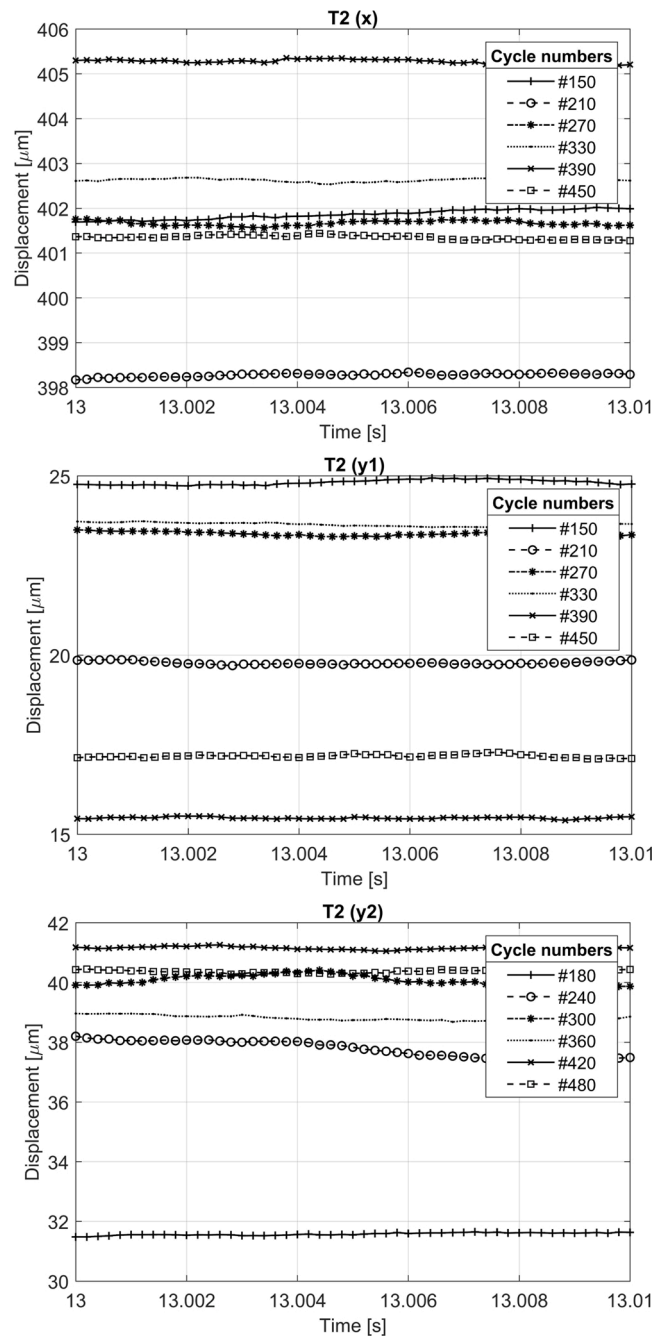


Fig. 11. Mold's plates displacement – T2.

The graphs of the total mold displacement for both cavity and core retainer plates are shown in Fig. 13. As can be seen, the plots show a maximum displacement of 105 and 94  $\mu\text{m}$  in cavity and core plates respectively. Although a significant displacement between both plates is found to exist, the relative displacement at each point of the plates needs to be calculated for the purpose of misalignment measurements.

To provide a means of measuring misalignment at each cavity, the nodes at the middle of each wall of targeted cavity were selected. The X and Y displacement for each selected node were recorded and the average from all displacements of the four nodes were computed for that cavity. Since Moldex3D utilizes the technique of matching elements, the corresponding nodes are available for calculation of the total displacement at the core side. The misalignment was obtained from the absolute difference of displacements on both plates at each cavity. After calculations, the misalignment for selected cavities with respect to the cavity

numbers illustrated in Fig. 2 can be seen in Fig. 14. In examining the graph, it is apparent that the maximum misalignment of 11  $\mu\text{m}$  occurred at the corners; lower right and upper left of the core side where the maximum total displacement was observed. Another observation is that thermal expansion had the least misalignment of 2  $\mu\text{m}$  at cavity numbers 17 and 16 where they are at the closest distance to the round guiding pillars. As was true for the displacement sensors, once again FE analysis showed that the misalignment caused by the thermal expansion of mold inserts is in the range of 10–12  $\mu\text{m}$ .

However, as previously shown, a significant dimensional error still exists in the length and width of molded parts. An additional observation from all graphs previously shown for dimensional variations is that the length and width of molded parts are below the nominal values. This implies that the molded parts tend to deform as seen in Fig. 15. More specifically, warpage may have caused the deformation of molded parts.



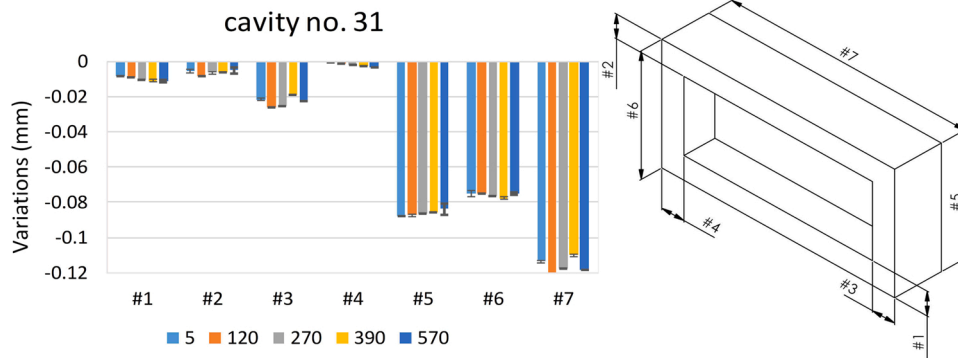


Fig. 12. Dimensional variations in cavity no. 31 – T2, error bars =  $\pm 1$  standard deviation, Max. standard deviation =  $3.1 \mu\text{m}$ .

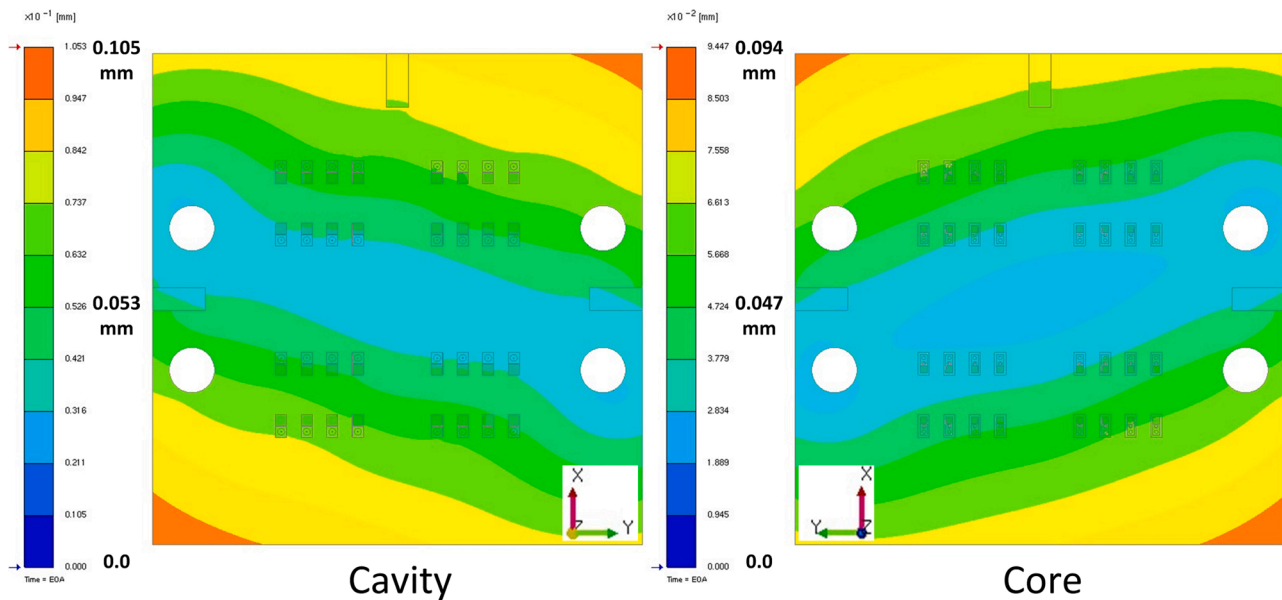


Fig. 13. Total displacement of cavity and core retainer plates.

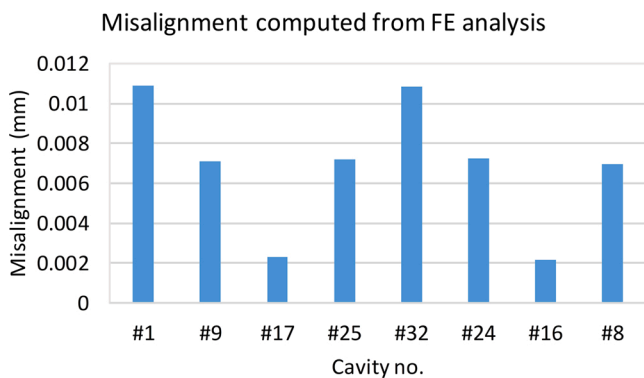


Fig. 14. Misalignment calculated from FE analysis for selected cavities.

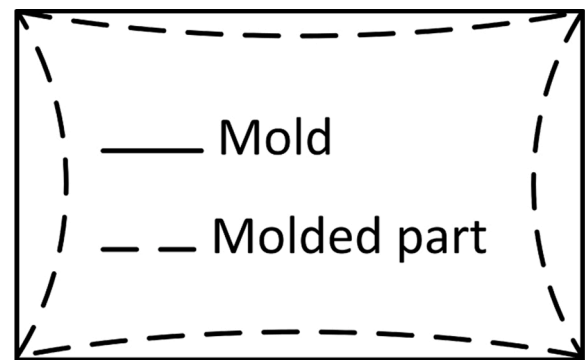


Fig. 15. Schematic deformation of the part after ejection from injection mold.

Therefore, a simulation was conducted for this analysis. The results of applying the conditions of molding process for warpage analysis are shown in Fig. 16.

Note that a detailed warpage analysis was not an aim of this research. The analysis described herein for warpage was used to indicate the source of error observed in the length and width of the molded parts. From Fig. 16, a displacement error of  $100 \mu\text{m}$  (yellow color zone) was

observed for each side of the part. When considering the warpage deformation for both sides, a total displacement of  $200 \mu\text{m}$  was calculated for the total length error, which was double that measured in the molded parts. The same occurred for the width when a displacement of  $74 \mu\text{m}$  can be seen from the analysis for one side. Both displacements obtained from the analysis proved to be as much as twice compared to dimensional variations observed on the molded parts. When looking at the part geometry used in the FE analysis, it becomes apparent that it

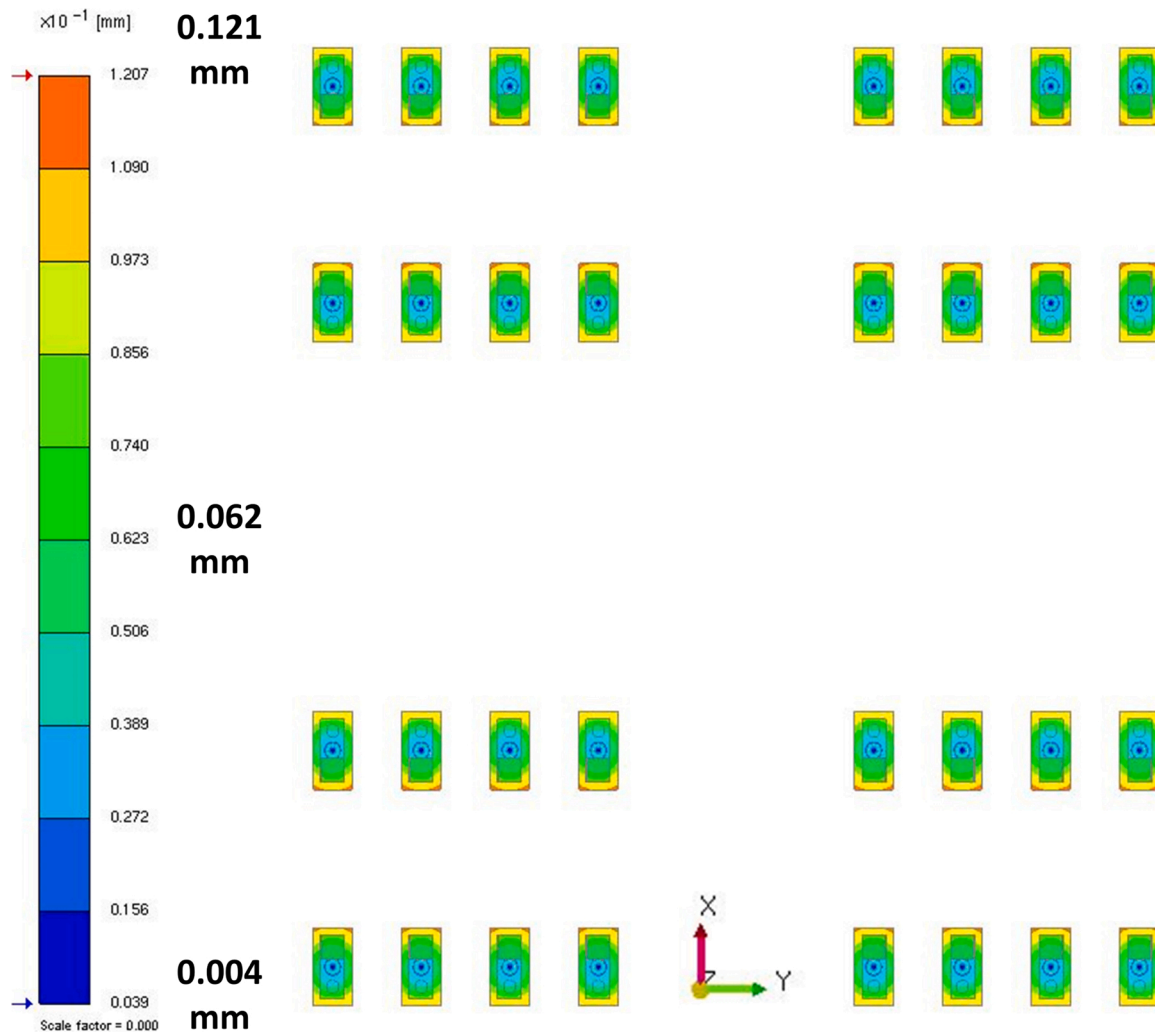


Fig. 16. Total deformation due to the level of warpage. (For interpretation of the references to color in this figure citation, the reader is referred to the web version of this article.)

came from 3D CAD, while it must be scaled up in the mold inserts to compensate for material shrinkage of the final molded part. This scaling was not considered in the analysis and can describe the differences of length and width error obtained from the analysis and measurements. Since the mold was not available for further measurements of the mold's cavities, the analysis was performed with the part geometry from a CAD model.

#### 4. Conclusion

The measurement method of inductance probes mounted on the sides of the mold was able to isolate and quantify the mold deflection as verified relative to dimensional variations of molded parts. Mold displacement at the parting plane can thereby be estimated precisely to be up to 12  $\mu\text{m}$  for the testing mold due to the thermal expansion, and is confirmed by FE simulation. The errors induced by milling and finishing of cavities and cores has a contribution to the extent of 10–15  $\mu\text{m}$ . The results from FE analysis however, seem to indicate that the warpage of the molded parts themselves played a greater role than the misalignment of mold's plates in determining their dimensional variations for the specific part geometry studied in this research. As stated previously, a further experiment is needed to fully prove this.

When comparing the results on the molded parts produced by the two injection molding machines with the same machine parameters, slight changes in dimensions of the parts were observed. While this

showed signs of a further error source due to the installation of the mold on a different injection molding machine, assembly and dismantling the inserts in cavity and core retainers, higher dimensional variations would be expected on the molded parts as it is observed in some tests of this research. Before using this result, it is highly recommended that more experiments be performed.

#### Acknowledgements

The work was funded by grant no. 5150-00021A, the Innovation Fund Denmark, acting under innovation consortium HASIM. The authors thank colleagues who provided insight and expertise that greatly assisted the research. Support from FlowHow® ApS for training and using Moldex3D is gratefully acknowledged.

**Conflict of interest:** None declared.

#### References

- [1] Chen Z, Turng L-S. A review of current developments in process and quality control for injection molding. *Adv Polym Technol: J Polym Process Inst* 2005;24(3): 165–82.
- [2] Lu X, Khim LS. A statistical experimental study of the injection molding of optical lenses. *J Mater Process Technol* 2001;113(1–3):189–95.
- [3] Chen S-C, Chang Y, Chang Y-P, Chen Y-C, Tseng C-Y. Effect of cavity surface coating on mold temperature variation and the quality of injection molded parts. *Int Commun Heat Mass Transfer* 2009;36(10):1030–5.

- [4] Kurt M, Saban Kamber O, Kaynak Y, Atakok G, Girit O. Experimental investigation of plastic injection molding: assessment of the effects of cavity pressure and mold temperature on the quality of the final products. *Mater Des* 2009;30(8):3217–24.
- [5] Kuek S-c. An investigation of cavity pressure as a process and quality indicator in the micro-injection molding process [Master's thesis]. Clemson University; 2007.
- [6] Attia UM, Alcock JR. Optimising process conditions for multiple quality criteria in micro-injection moulding. *Int J Adv Manuf Technol* 2010;50(5–8):533–42.
- [7] Farshi B, Gheshmi S, Miandoabchi E. Optimization of injection molding process parameters using sequential simplex algorithm. *Mater Des* 2011;32(1):414–23.
- [8] Park HS, Nguyen TT. Optimization of injection molding process for car fender in consideration of energy efficiency and product quality. *J Comput Des Eng* 2014;1(4):256–65.
- [9] Wang KK, Zhou J. A concurrent-engineering approach toward the online adaptive control of injection molding process. *CIRP Ann* 2000;49(1):379–82.
- [10] Chen Z, Turng L-S, Wang K-K. Adaptive online quality control for injection-molding by monitoring and controlling mold separation. *Polym Eng Sci* 2006;46(5):569–80.
- [11] Min BH. A study on quality monitoring of injection-molded parts. *J Mater Process Technol* 2003;136(1–3):1–6.
- [12] Chen X, Chen G, Gao F. Capacitive transducer for in-mold monitoring of injection molding. *Polym Eng Sci* 2004;44(8):1571–8.
- [13] Dubay R, Pramujati B, Han J, Strohmaier F. An investigation on the application of predictive control for controlling screw position and velocity on an injection molding machine. *Polym Eng Sci* 2007;47(4):390–9.
- [14] Lu N, Gao F. Stage-based online quality control for batch processes. *Ind Eng Chem Res* 2006;45(7):2272–80.
- [15] Gordon G, Kazmer DO, Tang X, Fan Z, Gao RX. Quality control using a multivariate injection molding sensor. *Int J Adv Manuf Technol* 2015;78(9–12):1381–91.
- [16] Tsai K-M, Lan J-K. Correlation between runner pressure and cavity pressure within injection mold. *Int J Adv Manuf Technol* 2015;79(1–4):273–84.
- [17] Zhang Y, Mao T, Huang Z, Gao H, Li D. A statistical quality monitoring method for plastic injection molding using machine built-in sensors. *Int J Adv Manuf Technol* 2016;85(9–12):2483–94.
- [18] Kitayama S, Yokoyama M, Takano M, Aiba S. Multi-objective optimization of variable packing pressure profile and process parameters in plastic injection molding for minimizing warpage and cycle time. *Int J Adv Manuf Technol* 2017;92(9–12):3991–9.
- [19] Masato D, Rathore J, Sorgato M, Carmignato S, Lucchetta G. Analysis of the shrinkage of injection-molded fiber-reinforced thin-wall parts. *Mater Des* 2017;132:496–504.
- [20] Carpenter B, Patil S, Hoffman R, Lilly B, Castro J. Effect of machine compliance on mold deflection during injection and packing of thermoplastic parts. *Polym Eng Sci* 2006;46(7):844–52.
- [21] Niewels J, Romanski Z, Arnott R. Method and apparatus for countering mold deflection and misalignment using active material elements. US Patent App. 10/830,434 (2005).
- [22] Huang C-C, Truong T-C, Chen S-H. An effective approach to measuring real-time mold deflection during injection molding. *J Polym Eng* 2011;31(8–9):549–60.
- [23] Huszar M, Belblidia F, Arnold C, Bould D, Sienz J. An exploration of core misalignment, shifting and deflection phenomena through thickness measurements on thin-walled injection moulded bins. *Sustain Des Manuf* 2014;Part 1:108.
- [24] Jung JT, Lee B-K. Fluid-structure interaction model to predict deformation of mold cores in injection molding filling stage. *J Mech Sci Technol* 2018;32(2):817–22.
- [25] Kazmer DO, Velusamy S, Westerdale S, Johnston S, Gao RX. A comparison of seven filling to packing switchover methods for injection molding. *Polym Eng Sci* 2010;50(10):2031–43.
- [26] Zhao P, Zhou H, He Y, Cai K, Fu J. A nondestructive online method for monitoring the injection molding process by collecting and analyzing machine running data. *Int J Adv Manuf Technol* 2014;72(5–8):765–77.
- [27] Ishikawa T, Ohshima M. Visual observation and numerical studies of polymer foaming behavior of polypropylene/carbon dioxide system in a core-back injection molding process. *Polym Eng Sci* 2011;51(8):1617–25.
- [28] Fleming AJ. A review of nanometer resolution position sensors: operation and performance. *Sens Actuators A: Phys* 2013;190:106–26.
- [29] Nguyen TK, Hwang CJ, Lee B-K. Numerical investigation of warpage in insert injection-molded lightweight hybrid products. *Int J Precis Eng Manuf* 2017;18(2):187–95.
- [30] Song Z, Liu S, Wang X, Hu Z. Optimization and prediction of volume shrinkage and warpage of injection-molded thin-walled parts based on neural network. *Int J Adv Manuf Technol* 2020;109(3):755–69.
- [31] Chang Y, Huang ST, Huang S-W, Chen S, Huang C, Chen M-C, et al. Warpage management using three dimensional thickness control method in injection molding. ANTEC plastic: annual technical conference proceeding 2009.
- [32] Nian S-C, Fang Y-C, Huang M-S. In-mold and machine sensing and feature extraction for optimized ic-tray manufacturing. *Polymers* 2019;11(8):1348.
- [33] Singh G, Verma A. A brief review on injection moulding manufacturing process. *Mater Today: Proc* 2017;4(2):1423–33.
- [34] Fernandes C, José Pontes A, Viana JC, Gaspar-Cunha A. Modeling and optimization of the injection-molding process: a review. *Adv Polym Technol* 2018;37(2):429–49.
- [35] Manoj M, Ansari MNM, Shanks RA. Review on the effects of process parameters on strength, shrinkage, and warpage of injection molding plastic component. *Polym Plast Technol Eng* 2017;56(1):1–12.
- [36] Annicchiarico D, Alcock JR. Review of factors that affect shrinkage of molded part in injection molding. *Mater Manuf Process* 2014;29(6):662–82.
- [37] STRACK NORMA GmbH. Strack standard parts, W21 Guide pillar. <https://www.strack.de/en/shop/?idm=2297&d=1&idmp=95> [accessed 19 June 2019].
- [38] STRACK NORMA GmbH. Strack standard parts, Z51-0 Centering element. <https://www.strack.de/en/shop/?d=1&idmp=94&idm=2456> [accessed 19 June 2019].
- [39] GF Machining Solution. Precision of the highest level. [https://www.gfms.com/county\\_SG/en/mikron-mill-p-500-u/application-report.html](https://www.gfms.com/county_SG/en/mikron-mill-p-500-u/application-report.html) [accessed 26 August 2020].